Performance of a Multimode Photon-Counting Optical Receiver for the NASA Lunar Laser Communications Demonstration

M.M. Willis, A.J. Kerman, M.E. Grein, J. Kansky, B.R. Romkey, E.A. Dauler, D. Rosenberg, B.S. Robinson,
D.V. Murphy, D.M. Boroson

MIT Lincoln Laboratory
244 Wood St.
Lexington, MA 02420

Abstract—In this talk, we describe recent measurements of the optical detector subsystem of the ground receiver to be deployed for the NASA Lunar Lasercom Demonstration (LLCD). The primary mission objective is to demonstrate a two-way selectable data rate communications link between a ground station and an optical terminal on a lunar orbiting spacecraft commissioned for the Lunar Atmosphere and Dust Environment Explorer (LADEE). A secondary goal is to demonstrate two-way time of flight measurements between the terminals with sub-cm resolution using the optical data communications channel. The focus of this talk will be on the optical performance of the downlink between the spacecraft (transmitting a ~ 0.5 W average power beam near 1550 nm from a 10-cm aperture with 16-ary pulse position modulated data stream) and the optical receiver on the ground terminal. Laboratory tests of the optical receiver performance with an incident PPM signal with ~5-GHz time slots and ½-rate serially-concatenated PPM forward error-correction coding showed error-free performance at 38-622 Mb/s with a receiver sensitivity of 1-2 incident photons/bit.

Index Terms—laser communication, pulse position modulation, PPM, photon counting, LLCD

I. SYSTEM OVERVIEW

The Lunar Laser Communications Demonstration (LLCD) aims to demonstrate multi-rate (up to 622 Mbps user data rate), high-sensitivity, free-space communications between a lunar satellite and Earth-based ground terminal [1]. Fig. 1 shows a block diagram of the photon-counting downlink receiver. Although this paper provides the high-level technical detail needed to motivate many of the receiver design choices, it serves primarily to present the preliminary, empirically measured downlink communications performance for the ground terminal receiver as built and tested in a pre-mission, laboratory environment. More detailed explanations of the space terminal transmitter, ground terminal receiver, and downlink synchronization algorithms can be found in [2-4].

Tight size/weight/power constraints on the satellite payload (the average optical transmit power is < 1 W), in addition to the large R^2 link loss due to the approximately 400 thousand kilometer separation between the earthbound ground terminal and lunar satellite, necessitate efficient usage of the optical signal appearing at the ground terminal receiver. Some constraints on the collection optics for LLCD are that: 1.) they be simple and relatively compact and transportable to support relocation on short notice--this feature initially provided flexibility in postponing the final ground terminal site selection in order to optimize mission link availability depending on the expected seasonal cloud coverage at launch time; and, 2.) they mitigate communications performance degradation on days with strong atmospheric turbulence. The receiver collection optics consist of four 40-cm telescopes mounted to a gimbal and aligned to a common bore-sight; the use of multiple telescopes provides spatial diversity to reduce the severity of atmospheric-induced fades; the use of a common, fixed bore-sight eliminates the need for dynamic, orientation-dependent deskew and synchronization procedures to time align signals across the telescope array. A clamshell enclosure protects these telescopes from the weather during periods of inactivity. Light from each telescope is guided by a weakly polarization-maintaining multimode optical fiber (MMPMF), and lens coupled onto a 14 micron diameter array of four interleaved superconducting nanowire single-photon detectors (SNSPD)—this passive and relatively simple multimode scheme maintains high coupling efficiency in the presence of strong turbulence without the need for adaptive optics. Each of the total sixteen detector elements is independently biased and cooled to 2.6K inside a closed-cycle cryostat to achieve detection efficiencies of ~60% per nanowire as measured from the input to the MMPMF. Fast reset times (~15 ns) and small timing jitter (~60 ps FWHM) allow the SNSPD-based photon counting receiver to achieve high count rates with relatively few detector elements when compared to other technologies with similar detection efficiency. The nanowire geometry seen in Fig. 2, which resembles a wire grid, results in a 3-4 dB reduction in detection efficiency for fields polarized perpendicular to the wires; thus, polarization alignment between the multimode fiber and detector sample is required.

The output electrical pulses from the detectors are conditioned first by cryogenic GaAs HEMT amplifiers packaged in proximity to the detectors on the sample mount at
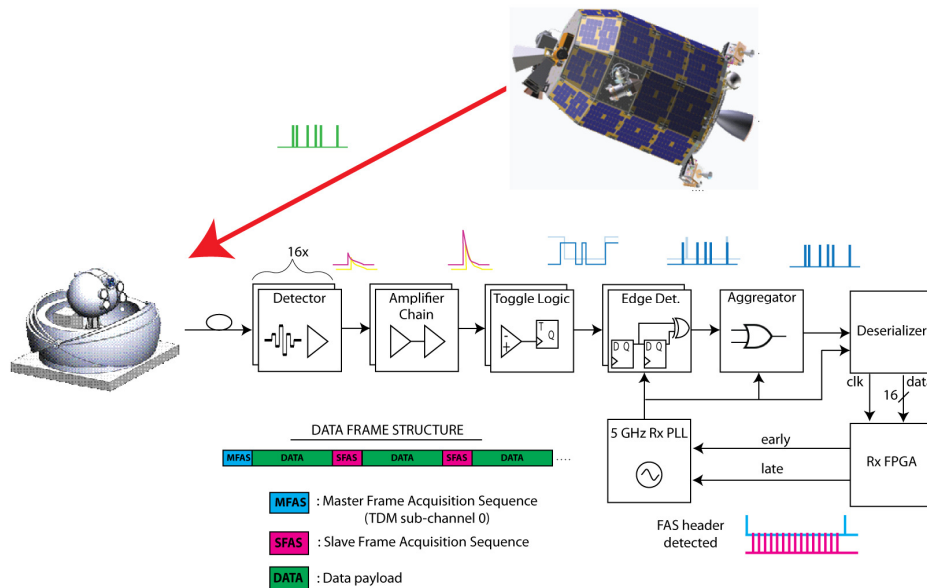
Figure 2: LLCD Downlink Block Diagram

2.6K, and then subsequently by two additional stages of amplification at room temperature, outside of the refrigerator. The amplified waveforms pass through a one bit analog-to-digital converter (i.e., comparator) whose discrimination threshold is determined empirically to maximize SNR. Downstream, a toggle flip-flop performs asynchronous rising edge detection on this digital waveform and feeds the result into a two-bit shift register with cascaded XOR gate for synchronization with a master 5 GHz slot clock. These synchronized outputs from the four channels within each telescope are aggregated once with synchronous 4:1 OR-based logic at the telescope level, and then again across telescopes to perform an effective 16:1 OR-based synchronous collapse of all channel outputs to one detected photon time of arrival data stream. This OR-based aggregation using digital logic offers significant simplification by reducing the number of high-speed signal traces and eliminating the need for high-speed slot counting logic, at the expense of the ability to resolve multiple detection events per slot. This tradeoff does not degrade performance appreciably in the targeted low-flux, high receiver sensitivity regime (~ 1 photon/bit) where the expected mean photon number per slot does not differ much from one.

After digitization and aggregation, a high-speed 16:1 demultiplexer parallelizes the photon arrival data stream (5 GHz frequency at 1 bit wide) into a slower one (311 MHz frequency at 16 bits wide) that is more amenable to processing within a six FPGA back-end processor. A basic understanding of the downlink frame structure alluded to pictorially in Fig. 1 is helpful for understanding further system functionality. Due to the numerous erasures introduced by the photon-counting channel, a strong forward error-correcting code is needed to close the link. Decoding operations are block-based and require precise delineation of the codeword boundaries; this is achieved through insertion of periodic frame acquisition sequences (FAS) into the downlink stream to separate codewords using time-division multiplexing (a "master" FAS is further used to distinguish TDM sub-channel 0 from other channels marked with a "slave" FAS). In addition to establishing codeword boundaries, pattern recognition of the FAS headers within the receiver is used to establish PPM slot boundaries and demodulate symbols, compute the Tx/Rx phase error used to drive the symbol clock phase-lock loop (PLL), as well as track channel variations by monitoring the un-coded symbol error rate. The gateway FPGA performs all of these functions, in addition to decimating the input data stream across multiple data rates and logging telemetry from supporting receiver electronics. The remaining five FPGAs are used to implement the deinterleaving and decoding algorithms. The downlink uses a rate-1/2, serially concatenated pulse position modulation decoder originally developed at JPL [5]. The iterative nature of this soft decision decoding algorithm is computationally intensive; our multi-FPGA decoder implementation supports a maximum real-time decoded throughput of 155 Mbps. This can be configured to demodulate, for example, ¼ of the subchannels at the highest rate, 622 Mbps.
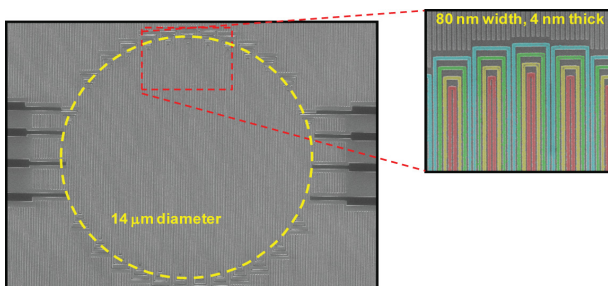

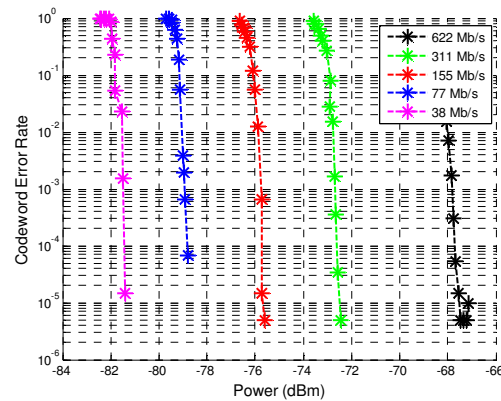Figure 1: Four Element Superconducting Nanowire Detector Array

Figure 3: Codeword Error Rate Curve

II. EXPERIMENTAL RESULTS

Fig. 3 shows the measured codeword error rate performance at all supported downlink rates for the receiver as built including the sixteen element detector array, readout electronics, and digital processors (but excluding the telescope optics--the Tx/Rx are fiber, and not free-space, coupled, during laboratory characterizations), and operating under autonomous clock acquisition and recovery. Table 1 summarizes the "error-free" communications thresholds (defined at the 10^{-4} codeword error rate where the curve is sharp but each point is still measurable using manageable integration periods of tens of seconds). Additional optimizations are under way.

Data Rate (Mb/s)	Comm. Threshold (dBm)	Sensitivity (photons/bit)
622	-67.85	2.05
311	-72.63	1.36
155	-75.72	1.34
77	-78.85	1.3
38	-81.5	1.45

Table 1: Receiver Sensitivity

III. CONCLUSION

Scheduled to launch in 2013, the Lunar Laser Communications Demonstration will be NASA's first optical communications demonstration. To date in the laboratory we have demonstrated reliable performance of a novel multimode photon-counting receiver employing superconducting nanowire detector technology, at rates of 38, 77, 155, 311, and 622 Mbps with sensitivity approaching 1-2 incident photons/bit.

REFERENCES

[1] D.M. Boroson, J.J. Scozzafava, D.V. Murphy, B.S. Robinson, H. Shaw, "The lunar laser communications demonstration," Space Mission Challenges for Information Technology, 2009, p 23-28, 19-23 July 2009.

[2] Grein, M.E.; Kerman, A.J.; Dauler, E.A.; Shatrovoy, O.; Molnar, R.J.; Rosenberg, D.; Yoon, J.; DeVoe, C.E.; Murphy, D.V.; Robinson, B.S.; Boroson, D.M.; , "Design of a ground-based optical receiver for the lunar laser communications demonstration," Space Optical Systems and Applications (ICSOS), 2011 International Conference on , pp.78-82, 11-13 May 2011.

[3] Willis, M.M.; Robinson, B.S.; Stevens, M.L.; Romkey, B.R.; Matthews, J.A.; Greco, J.A.; Grein, M.E.; Dauler, E.A.; Kerman, A.J.; Rosenberg, D.; Murphy, D.V.; Boroson, D.M.; , "Downlink synchronization for the lunar laser communications demonstration," Space Optical Systems and Applications (ICSOS), 2011 International Conference on , pp.83-87, 11-13 May 2011.

[4] S. Constantine, L. Elgin, M.L. Stevens, J.A. Greco, K. Aquino, D.D. Alves, B.S. Robinson, "Design of a High-Speed Modem for the Lunar Laser Communications Demonstration," Proc. SPIE 7923, 792308 (2011).

[5] B. Moision, J. Hamkins, "Coded Modulation for the Deep-Space Optical Channel: Serially Concatenated Pulse-Position Modulation," IPN Progress Report 42-161.